

Quantifying the Predictability of Winter River Flow in Iberia. Part II: Seasonal Predictability

SONIA GÁMIZ-FORTIS

Departamento de Física Aplicada, Universidad de Granada, Granada, Spain, and NCAS-Climate, Department of Meteorology, University of Reading, Reading, United Kingdom

DAVID POZO-VÁZQUEZ

Departamento de Física, Universidad de Jaén, Jaén, Spain

RICARDO M. TRIGO

CGUL, IDL, University of Lisbon, and Departamento de Engenharias, Universidade Lusófona, Lisbon, Portugal

YOLANDA CASTRO-DÍEZ

Departamento de Física Aplicada, Universidad de Granada, Granada, Spain

(Manuscript received 15 November 2006, in final form 30 August 2007)

ABSTRACT

The role of the Atlantic summer and autumn SSTs on the predictability of the winter Iberian Peninsula river flows is analyzed during the period 1923–2004. The analysis is based on the results of an interannual predictability experiment, using autoregressive-moving-average (ARMA) models, carried out in the first part of this work. A standard principal component analysis (PCA) was applied to the summer and autumn SST fields for the entire Atlantic Ocean. Then, the association between the resulting principal component (PC) series and the Iberian Peninsula streamflow series was analyzed, in order to use the PC series as additional predictor variables in a seasonal forecasting regression model. Results proved, first, that during autumn, the SST variability in the so-called North Atlantic horseshoe pattern has a statistically significant linear influence in the following winter streamflow values. In particular, the use of this SST information considerably improves the skill of the linear forecast (improvements against climatology range from 61% to 90%) compared to the ARMA-alone model (51%–53%). These improvements are mostly related to the ability of the SST information to provide better estimates of extreme streamflow values. Additionally, results showed that the summer tropical Atlantic and the autumn southwestern Atlantic SST variability have a significant nonlinear influence on the following winter streamflow values. In particular, there is a tendency for negative streamflow anomalies following tropical Atlantic summer negative SST anomalies and following southwestern Atlantic autumn SST positive anomalies. It is finally concluded that the linear interannual predictability of the Iberian Peninsula winter streamflow is greater (two-thirds of the total predictability) than the predictability associated with the previous season autumn SSTs (one-third).

1. Introduction

It is commonly accepted that the skill of seasonal to interannual climate forecasts originates from slowly varying components of the climate system, such as the

snow cover and SST spatial distribution, rather than the initial state of the atmosphere, which is more important in shorter time forecasts. Regarding the SST, it is commonly accepted that there are two different ways in which the ocean can influence the atmosphere and give rise to low frequency variability in climatic variables like temperature or precipitation, and, therefore, in the streamflow. The first is through fully ocean–atmosphere coupled modes, such as the well known El Niño–Southern Oscillation (ENSO) phenomenon (e.g.,

Corresponding author address: David Pozo-Vázquez, Departamento de Física, Universidad de Jaén, Campus Lagunillas, Edif. A3, 23071, Jaén, Spain.
E-mail: dpozo@ujaen.es

Rasmusson and Carpenter 1982). The main influence of this phenomenon is confined to the equatorial Pacific region, although there is some evidence of a weak ENSO influence in the North Atlantic region (Wilby 1993; van Oldenborgh et al. 2000; Pozo-Vázquez et al. 2001, 2005; Mariotti et al. 2002; Vicente-Serrano 2005). Regarding the most important large-scale circulation mode in the North Atlantic region, the North Atlantic Oscillation (NAO), it is not clear, still today, whether or not it is a coupled phenomenon (Rodwell et al. 1999). The second way is a stochastic process, that is, the inertial response of the atmosphere to the ocean. This second possibility is based on the existence of a special resonance mechanism, that is, the existence of certain frequencies that are particularly efficient at transferring energy from the ocean to the atmosphere. Seasonal statistical climate forecasting models take advantage of all these types of influences of SST on the land surface climate making use of lag-lead relationships between the oceanic and land surface conditions (Colman and Davey 1999; Rodwell and Folland 2002; Phillips and McGregor 2002; Lloyd-Hughes and Saunders 2002). The relationship between the NAO and the climate of the North Atlantic region is maximum with no lag. But the prospect for seasonal predictability of this phenomenon (Rodwell et al. 1999; Saunders and Qian 2002) has also led to the possibility of including the NAO index in the statistical climate forecasting models (e.g., Rodriguez-Fonseca and de Castro 2002; Saunders and Qian 2002; Wilby 2001). Evaluation of these statistical seasonal forecast tools suggests that the best statistical models currently perform as well as, if not better than, the best dynamical models in the northern extratropics.

Streamflow reflects the influence of a certain number of parameters, namely, precipitation, evapotranspiration, and other hydrological cycle components, together with anthropogenic influences. The nature of the relationship between the climatic regimes over a river basin and its hydrological response, through its streamflow, presents different grades of complexity according to the physical characteristics of the basin. However, there are some objective reasons to prefer streamflow over precipitation for studying the impacts of climate variability on regional hydrology. First, the streamflow integrates the climatic forcings mentioned above; this may intrinsically emphasize the low-frequency components of the climate system (Rajagopalan et al. 1998). Additionally, the streamflow originates in the naturally filtered precipitation, which is less prone to contamination by space-time noise (Piechota et al. 1997). Advances in computing power, coupled with increased data availability, have led to a recent revolution in seasonal

streamflow forecasting. In particular, seasonal forecasts of streamflows are issued by a number of researchers, mainly in the United States, using both dynamical and statistical approaches (Redmond and Koch 1991; Liang et al. 1994; Nigam et al. 1999; Hartmann et al. 2002). Some attempts to forecast the river flow using statistical techniques have also been carried out in Europe. For instance, Wedgbrow et al. (2002) analyzed the dependence of the river flows in England on several climatic variables (as climatic indices and SST) and its usefulness to forecast the summer river flow for several rivers in England. In a recent work, Wilby et al. (2004) carried out a seasonal forecast of the river Thames flow using SSTs (among other) variables. Similarly, Rimbu et al. (2004) found that the summer and spring Danube River flow can be partially predicted using the previous winter SSTs of certain areas of the Pacific and Atlantic. In this latter case, validation results showed considerable improvement in the skill against climatology. Recently, seasonal climate forecast from the Development of a European Multimodel Ensemble System for Seasonal-to-Interannual Prediction (DEMETER) project has been used to obtain streamflow seasonal dynamical forecasts for South America (Coelho et al. 2006).

In summary, over midlatitudes, and particularly over Europe, the skill of seasonal streamflow forecasting models is relatively low, but potentially better than the skill associated with seasonal models for temperature or precipitation.

In the companion paper (Gámiz-Fortis et al. 2008, hereinafter Part I) an analysis of the interannual variability and predictability of the winter streamflow of the three most important international Iberian Peninsula rivers—the Douro, Tejo, and Guadiana—was carried out. In this second paper (Part II), the effort will be concentrated on potential added value of including Atlantic Ocean SST in the seasonal predictability of these streamflow series. This analysis is based on the results obtained with the interannual predictability experiment carried out in Part I. Here, the main aim is to evaluate any increment in winter streamflow forecasting skill attributable to the Atlantic summer and autumn SST that the interannual forecasting model (Part I) was not able to capture.

To this end, the residual time series resulting from the interannual forecasting experiment have been analyzed. This methodology allows, first, comparing the relative importance of the seasonal against interannual predictability and, second, constructing a statistical forecasting model that includes both seasonal and interannual sources of predictability.

This work is organized as follows: section 2 explains the data and methodologies used in this study. Section

3 deals with the results of the seasonal forecast and is divided into three parts: section 3a, which presents the analysis of the Atlantic SST data using principal component analysis (PCA); section 3b, which presents the results of the linear and nonlinear relationships between the SST and the streamflow series; and section 3c, which presents the results of a forecasting experiment that simultaneously includes both the interannual autoregressive-moving-average (ARMA) models and the seasonal regressions models. Finally, a discussion of the results and some conclusions are provided in section 4.

2. Data and methods

Three new time series have been obtained by subtracting the ARMA forecasts computed in Part I from the raw streamflow series. Note that these time series provide some kind of “residual” time series that contains the “information” that the interannual ARMA model was not able to capture. We will call, hereafter, these new time series Douro_ARMA, Tejo_ARMA, and Guadiana_ARMA.

To relate large-scale coherent modes of variability over the Atlantic Ocean and streamflow variability, an analysis of the spatiotemporal variability of the Atlantic Ocean SST is carried out using the PCA technique. The aim of this analysis is to find coherent pan-Atlantic summer and autumn spatiotemporal SST patterns able to provide some new sources of predictability for the following winter Iberian Peninsula river streamflow. Then, the corresponding time series associated with these patterns can be eventually incorporated into the framework of the linear regression model.

A monthly mean SST dataset over the Atlantic Ocean between 40°S and 80°N was used in this study. The data were derived from the Met Office Hadley Centre for Climate Prediction and Research for the period from January 1923 to December 2004. The original 1° latitude \times 1° longitude data grid is first transferred onto a 2° latitude \times 2° longitude grid by averaging all available data in the 2° \times 2° box. Monthly anomalies over the period 1923–2004 (total period) were constructed by subtracting the mean seasonal cycle from the monthly data. Finally, summer [June–August (JJA)] and autumn [September–November (SON)] seasonal averages were obtained from these deseasonalized series.

The PCA was applied to the correlation matrix of the SST field mentioned above. There is no single criterion that can be used to choose the number of principal components that ought to be retained in any given situation (Wilks 1995, chapter 9). It is a common procedure

to retain all variables until the total explained variance reaches a certain threshold (e.g., 70%). Another possibility is to retain all PCs that individually account for more variation than the average variation in the original dataset, that is, to keep all principal component (PC) series with corresponding eigenvalues higher than unity (Kaiser’s rule). Such empirical rules are, by their very nature, subjective and can lead to different interpretations by different authors (Trigo and Palutikof 2001). In the present analysis an objective rule was applied, based on what is hopefully a more reliable statistical approach. The objective “N rule” divides the total variability into “signal” and “noise” components (North et al. 1982; Preisendorfer 1988). Following this rule, the first five components were retained.

In the following step, a correlation analysis was conducted between the residual time series and the principal component SST series obtained in the previous analysis. Based on the results of this analysis, a linear regression model was constructed in order to forecast the residual time series. The Atlantic SST PC series were used as predictor variables. A similar cross-validation procedure as the one employed in Part I has been applied in this work. The period from 1923 to 1985 is used for training the Douro and Tejo models, while the shorter available period from 1947 to 1985 was used for the Guadiana. Again, data from 1986 to 2004 is used for validation purposes in all three river basins. Finally, the interannual forecasting model obtained in Part I and the seasonal forecasting regression model were integrated into a single forecasting model and its performance tested against raw streamflow values.

As mentioned in the introduction, this work aims to evaluate the increment in the winter streamflow forecasting skill attributable to the Atlantic previous summer and autumn SST, and that the interannual forecasting model (Part I) was not able to capture. There are other methodologies that could be applied to this end. One that is particularly valuable is the use of the autoregressive moving average with exogenous variables (ARMAX) models (Box and Jenkins 1976; Hipel and Mcleod 1994). These models allow inclusion of a regression with an external variable within the framework of the ARMA model. Therefore, the ARMAX models may be used to evaluate the interannual predictability (contained in the history of the series and accounted for by the ARMA part of the model) and the seasonal predictability (provided by the Atlantic SST and accounted for by the external variable regression). In this work we preferred the above-described methodology, obtaining first the ARMA interannual models of the streamflow series and then analyzing the resulting residuals for evaluating the seasonal predictability pro-

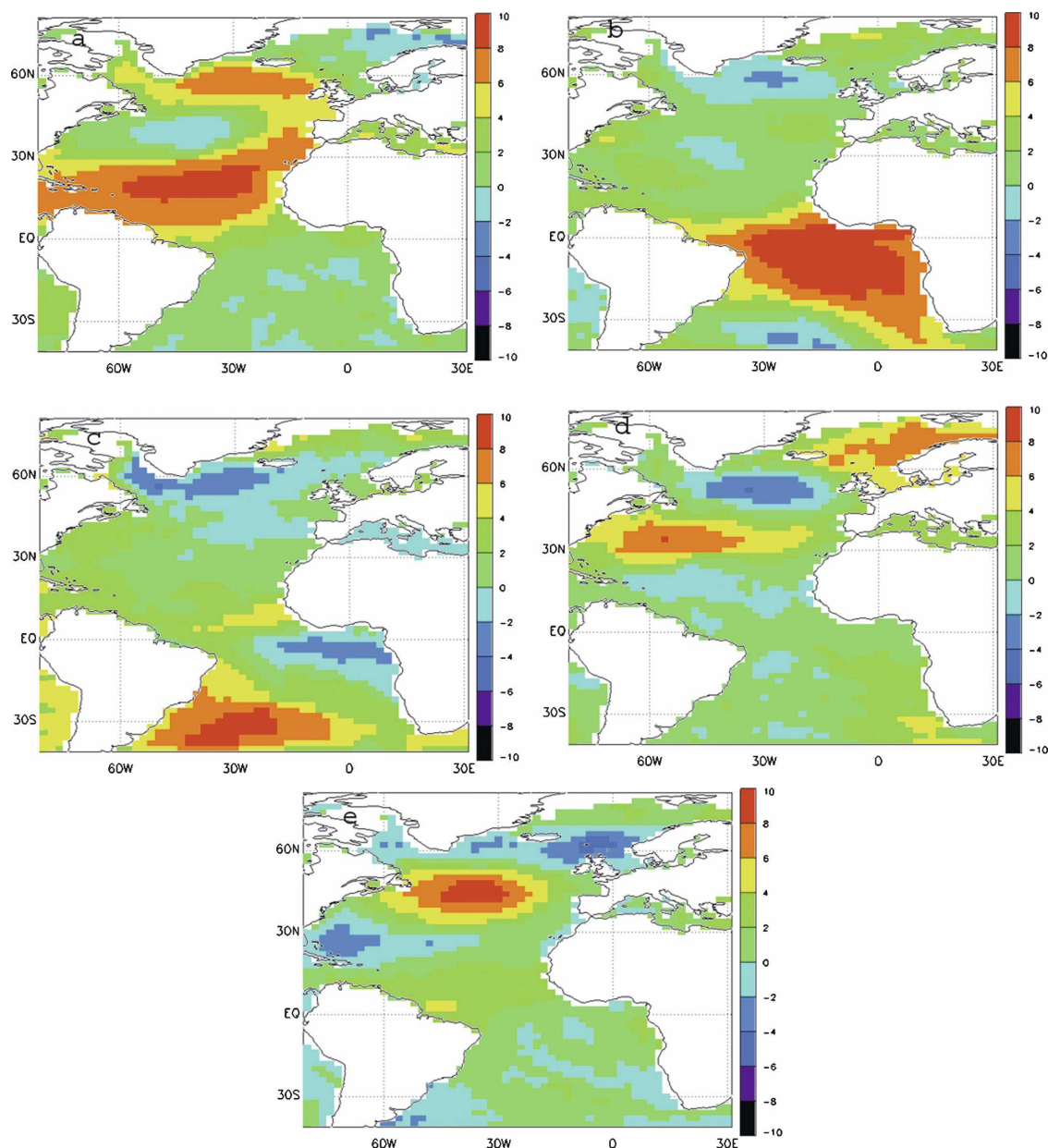


FIG. 1. Loading factors (by 10) for the (a) first, (b) second, (c) third, (d) fourth, and (e) fifth spatial modes resulting from a PCA of the Atlantic summer (JJA) sea surface temperature. The period of analysis is 1923–2004.

vided by the SST. The main advantage of this methodology is that it allows evaluating, independently, the interannual and the seasonal predictability of the streamflow series, while the ARMAX models provides an evaluation of, simultaneously, both sources of predictability. In particular, since the ARMAX model parameter estimation process takes into account the cross-correlations between the interannual and seasonal variables, it will be difficult to quantify the predictability arising independently from these two sources.

3. Analysis

a. Analysis of the Atlantic SST patterns

In this section, the spatiotemporal variability of the Atlantic Ocean SST is studied through the application of a PCA analysis to both summer and autumn Atlantic SST. The PCA reveals the existence of five significant modes of variability for both seasons. Figure 1 shows the spatial loading patterns or empirical orthogonal functions (EOFs) relative to the summer season. The combined variance associated with these five patterns

accounts for circa 60% of total the variance. The first mode (Fig. 1a), which explains 17% of the variance, shows a tripole pattern in the North Atlantic section, having positive loading centers in the high latitudes around 60°N, extending from the subpolar gyre to the Labrador Sea, and around 20°N, near the western coast of Africa, and a negative loading center around 35°N. This pattern is commonly called the North Atlantic horseshoe pattern and is described, for instance, in Czaja and Frankignoul (2002). The associated temporal series (not shown) presents some periods dominated by negative values (1901–30 and 1970–90) while the intermediate period (1930–70) is dominated by positive values. The second mode (Fig. 1b) explains 16% of the total variance and represents the SST variability in the tropical Atlantic. The highest loadings are found between the equator and 30°S. The associated temporal series S-PC (not shown) shows some short periods with trends, and considerable variability. The third mode (11% of explained variance, EV hereinafter), shown in Fig. 1c, can be associated with the southwestern Atlantic area (near Brazil) variability, in opposition with the Gulf of Guinea and the North Atlantic Ocean, near Greenland, but the loading factor is considerably lower. The slope of the associated temporal series (not shown) shows a steep upward trend from the mid-1960s to the beginning of the 1980s. From 1970 onward, positive anomalies can be found most of the time. The fourth mode (9% of EV), shown in Fig. 1d, presents a tripolar spatial pattern in the North Atlantic area, with centers of action southward (and with opposite signs) from those describing for the first mode. In particular, two negative anomaly centers are found to the southwest of Iceland and around 15°N latitude, while the positive anomaly center is located at about 30°N latitude. The corresponding temporal series (not shown) shows a considerable upward trend from 1920 to the beginning of the 1960s. Finally, the fifth mode (Fig. 1e, 6% of EV) shows an extensive area of high loading factor in the central North Atlantic region. The main feature of the associated temporal series (not shown) is a notably interdecadal variability between 1930 and 1960 and at the end of the record.

The PCA of the autumn SST shows very similar results. Therefore, five significant spatial patterns were found, explaining, respectively, 17%, 16%, 10%, 9%, and 9% of the variance. The associated spatial patterns are shown in Fig. 2. These patterns are very similar to those found for summer, the main differences being related to the order of importance. The first pattern for autumn (Fig. 2a) shows the spatial distribution of the second pattern for summer (Fig. 1b), while autumn's second pattern (Fig. 2b) corresponds to the spatial dis-

tribution of the first one during summer (Fig. 1a). The third autumn pattern (Fig. 2c) shows the same spatial pattern as the third summer pattern (Fig. 1c). Finally, the fourth autumn pattern (Fig. 2d) corresponds to the fifth summer pattern (Fig. 1e), and the fifth autumn pattern (Fig. 2e) corresponds to the fourth summer pattern (Fig. 1d). The corresponding temporal patterns (not shown) present very similar structure to that of the summer.

b. Influence of the Atlantic SST patterns on the streamflow

1) LINEAR ANALYSIS

In this section we attempt to relate the large-scale coherent modes of variability found previously for the Atlantic Ocean with the three Iberian rivers streamflow variability. The time series associated with these oceanic patterns might, eventually, be incorporated into the framework of a multilinear regression model.

To achieve this goal, we start by computing the linear correlation coefficients between the time series representative of the five summer and autumn SST spatial modes of variability and the following winter residual streamflow series for the three rivers. Correlation coefficient values between the SST modes and the raw streamflow series was also computed. Table 1 shows the results obtained for different periods: 1930–85 for the Douro, 1931–85 for the Tejo, and 1953–85 for the Guadiana. Only the second autumn mode shows a statistically significant correlation with the three raw streamflow series as well as the corresponding three residual time series. Additionally, a stability analysis shows that the correlations were stable throughout the analyzed period. Correlation values are slightly higher for the Guadiana. There are other SST modes that show statistically significant correlation but only with one (or two) rivers. For instance, the first summer mode is significantly correlated with the Douro and Guadiana, although with values lower than those obtained with the second autumn mode. River Guadiana also shows significant correlation values with the third summer PC, while the Tejo and Douro present significant correlation values with the third autumn PC. However, a stability analysis showed that these correlations were not stable when we considered the entire analyzed period.

Based on the previous results, we have developed three linear regression models in order to study the seasonal predictability of each streamflow. The models were fitted to the residual time series Douro_ARMA, Tejo_ARMA, and Guadiana_ARMA. From the previous correlation analysis we have proved that only the second autumn PC provides a statistically significant

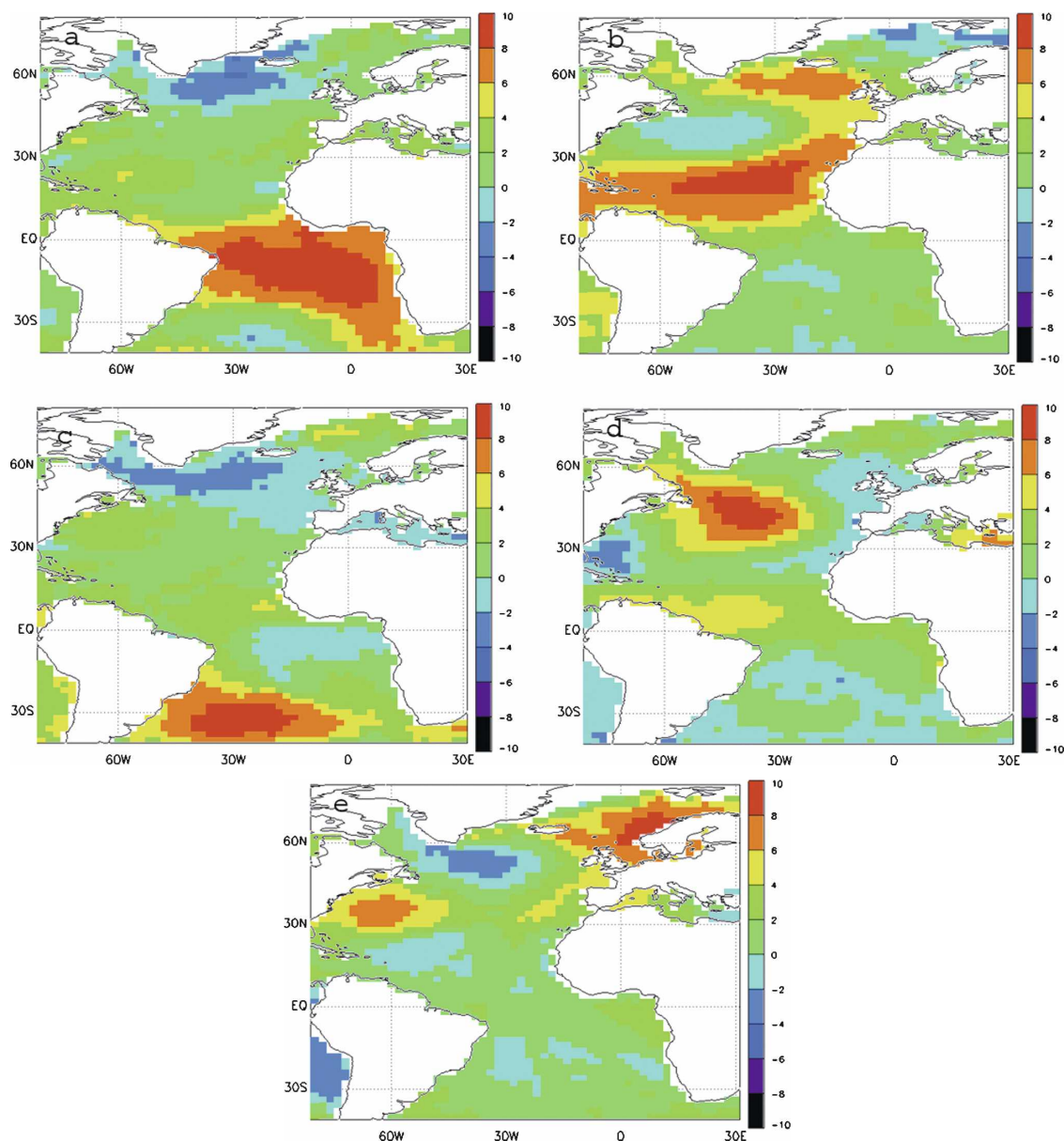


FIG. 2. As in Fig. 1, but for the autumn (SON) SST data.

source of predictability for the three analyzed streamflows. According to results from Table 1 some of the remaining PCs might also provide some predictability, albeit lower and dependent on the river. An approach to filter out local dependences and obtain results as generally as possible is to retain only those PCs of SST that provide predictability for the three rivers. Therefore, the remaining analysis is based on the use of the most robust predictor; that is, only the second autumn SST mode was retained. To develop the model, the period 1930–85 was used for calibration for the Douro, the similar period 1931–85 for the Tejo, and the shorter period 1953–85 for the Guadiana. Again, in all the three

cases, the final period 1986–2004 was used for validation purposes only. These periods correspond to the ARMA calibration and validation periods used in Part I and were selected in order to combine both the ARMA and SST forecast (section 3c). The regression models fitted for the three rivers residual time series are as follows:

$$\text{Douro: Douro_ARMA} = 0.10 + 0.64(\text{PC2 autumn})$$

$$\text{Tejo: Tejo_ARMA} = 0.020 + 0.39(\text{PC2 autumn})$$

$$\text{Guadiana: Guadiana_ARMA} = -0.06 + 0.61(\text{PC2 autumn}).$$

TABLE 1. Results of the correlation analysis between the raw and residual streamflow time series and the SST PC series. Asterisks indicate statistical significance at the 95% confidence level.

	Douro raw	Douro_ARMA	Tejo raw	Tejo_ARMA	Guadiana raw	Guadiana _ARMA
Summer SST						
PC1	0.20*	0.22*	0.13	0.15	0.23	0.26*
PC2	0.04	0.05	0.04	−0.07	0.20	0.20
PC3	−0.17	−0.19	−0.16	−0.15	−0.25*	−0.25*
PC4	−0.01	−0.02	−0.04	−0.04	−0.07	−0.03
PC5	0.07	0.05	0.04	0.06	0.05	0.06
Autumn SST						
PC1	−0.07	−0.05	0.02	−0.15	−0.10	−0.05
PC2	0.34*	0.36*	0.34*	0.33*	0.36*	0.37*
PC3	−0.23*	−0.20*	−0.22*	−0.23*	−0.16	−0.19
PC4	0.10	0.02	0.07	−0.06	0.14	0.15
PC5	−0.02	0.07	−0.12	0.03	−0.02	0.05

Table 2 presents a summary of the skill of the models during the validation period 1986–2004. The mean square errors (MSEs) are relatively low. In particular, the obtained values are 0.12 for Douro and 0.11 for both Tejo and Guadiana. However, mean absolute errors (MAEs) are relatively high for the three rivers: 0.54, 0.37, and 0.96 for Douro, Tejo, and Guadiana respectively.

To assess skill of the forecasting linear regression models, the percentage of improvement in MSE over a climatology forecast ($SMSE_{cli}$) and over a persistence forecast ($SMSE_{pe}$) were computed. The maximum improvement is obtained for the Guadiana, where the model performs 82% better than climatology and 93% better than persistence. For the Douro the improvement is 67% against climatology and 87% compared to persistence. Finally, for the Tejo, the improvement against climatology is 62% and 76% against persistence. Overall, the improvements against persistence are higher than against climatology, denoting the strong interannual variability of the streamflows. The phase accordance is 90% for the Tejo and Guadiana and 78% for the Douro. It can then be concluded that the linear regression models show considerable skill, improving

notably the results of using climatology or persistence forecasts.

2) NONLINEAR ANALYSIS

In the previous sections we performed a simple linear correlation analysis in order to study linear dependences between the SST PC and the streamflow series. In this section an additional analysis is carried out to search for possible nonlinear relationships. This will be done in several steps: first, a correlation analysis between extreme values of the residual series and raw series was conducted in order to evaluate the relationship between these two time series. Results showed that for both the upper and lower terciles and for the three rivers, the series are highly correlated. Particularly, values ranging between 0.78 and 0.9 for upper tercile cases and between 0.72 and 0.9 for the lower tercile cases. Given this result, and for the sake of clearness, the subsequent nonlinear analysis was performed using the raw streamflow series instead of the residuals series. Second, the distribution of the raw January–March (JFM) streamflow series following upper and lower terciles of the summer and autumn SST PCs were computed. Also the “middle tercile cases”—that is, values

TABLE 2. Statistical results of the forecasting experiments carried out with the regression models. The models use the second autumn SST PC series as the predictor variable. Values correspond to the validation period 1986–2004.

	Douro_ARMA	Tejo_ARMA	Guadiana_ARMA
MSE	0.12	0.11	0.11
MAE	0.54	0.37	0.96
MSE_{cli}	0.37	0.29	0.63
MSE_{per}	0.98	0.46	1.93
$SMSE_{cli}$ (%)	67	62	82
$SMSE_{per}$ (%)	87	76	93
Phase accordance (%)	78	90	90

ranging between the upper and lower terciles—were analyzed. Note that these cases stand for the normal or reference behavior. The aim of the study was to determine if the distribution of the JFM streamflow values depends on the previous summer and autumn PC SST series in some nonlinear way, nondetected in the previous linear analysis. The analysis was undertaken independently for each of the SST PC series and each streamflow series by calculating the cumulative streamflow distributions corresponding to the upper, middle, and lower SST PC time series distribution.

Results proved that the second summer PC and the third autumn PC have a significant nonlinear influence on the following winter streamflow series. Figures 3 and 4 show, respectively, the cumulative distribution for the second summer and third autumn PCs. Regarding the second summer PC, which represents the tropical Atlantic, negative streamflow anomalies are more probable following negative SST anomalies than following normal or positive ones. This influence is present for all three rivers, but is more important for the Tejo and Guadiana. For instance, Fig. 3c suggests that the probability of negative streamflow for the Guadiana is above 90% if the second summer PC series value lies in the lower tercile. On the other hand, if the SST PC series value lies in the upper or middle tercile, the probability is around 60%. Similar values are found for the Tejo and Douro. This signal is also present for the first autumn PC, which presents a very similar spatial pattern to that of the second summer PCs, but the strength is weaker and has not been represented.

For the sake of completeness, a composite analysis was also carried out. In particular, the composite values of the JFM streamflow series were calculated for the winters following the upper, lower, and middle terciles of the second summer SST PC series. Results proved that the composite values following lower tercile SST anomalies were -0.15 for the Douro, -0.19 for the Tejo, and -0.30 for the Guadiana. On the other hand, for the middle and upper terciles, the values for all three rivers range between -0.02 and 0.1 . For the three rivers, the difference between the lower tercile SST composite values and that of the middle and upper terciles proved to be statistically significant at the 95% confidence level using an appropriate t test.

The third autumn SST PC series, mainly associated with the southwestern Atlantic area SST variability, provides forecasting information associated with its upper tercile, as derived from Fig. 4. In particular, the probability of negative streamflow values is above 80% for the three streamflow series if the third autumn SST PC value lies in the upper tercile. Additionally, in these circumstances, the probability of extreme negative

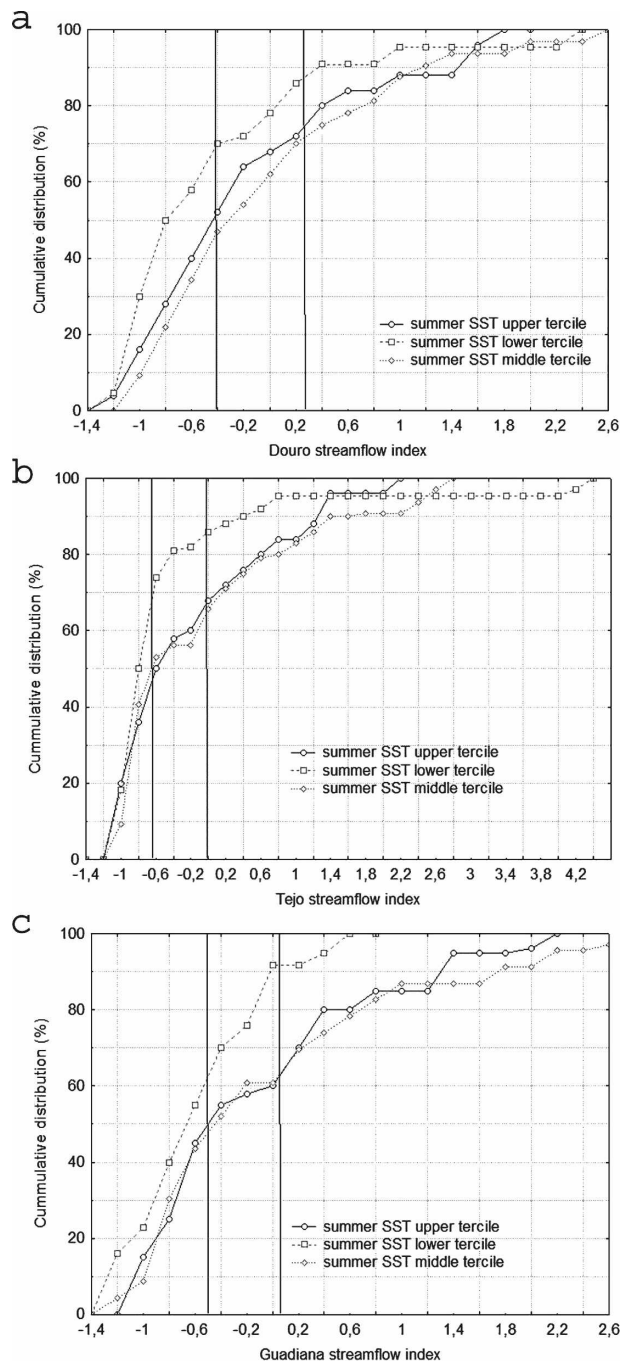


FIG. 3. Accumulated probabilities distribution of the raw winter (JFM) streamflow values following the upper, lower, and middle terciles of the second summer SST PC distribution for (a) Douro, (b) Tejo, and (c) Guadiana. Vertical lines indicate the location of the upper and lower terciles' values of the streamflow series.

streamflow values (lower streamflow tercile) is substantially higher than if the SST value lies in the middle or lower tercile. As in the summer case, composite values of the JFM streamflow series following the upper,

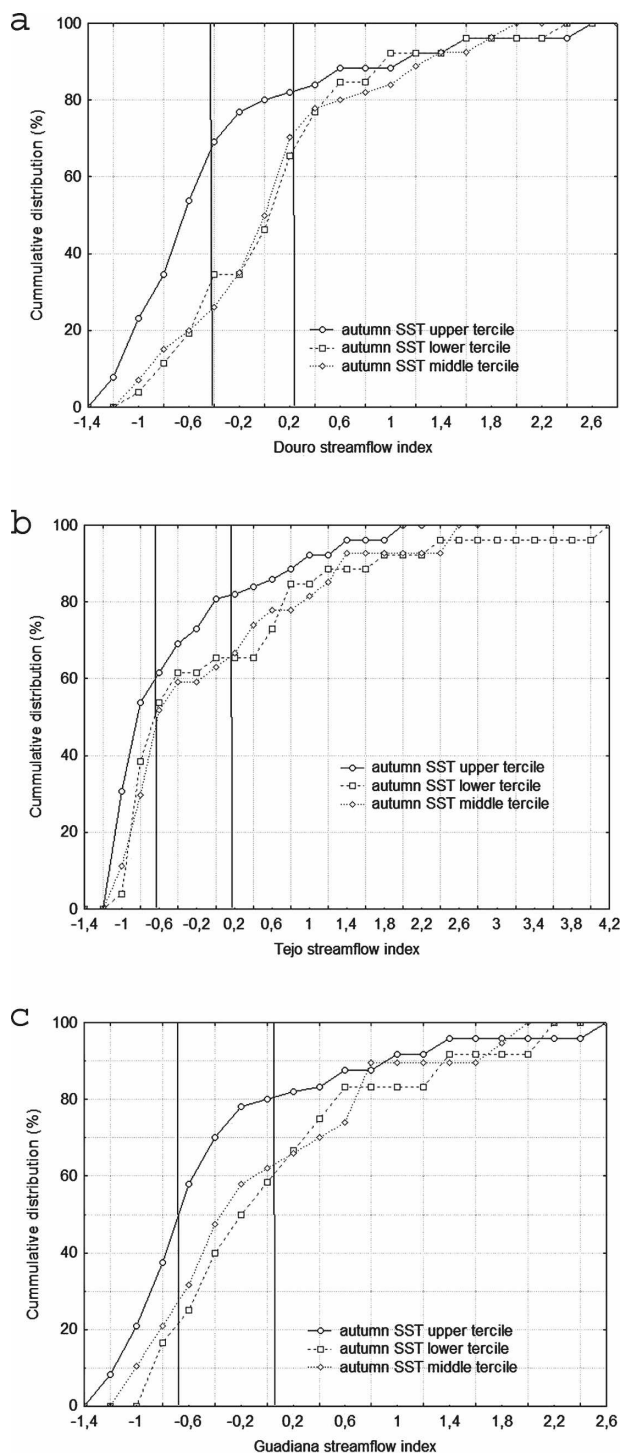


FIG. 4. Accumulated probabilities distribution of the raw winter (JFM) streamflow values following the upper, lower, and middle terciles of the third autumn SST PC distribution for (a) Douro, (b) Tejo, and (c) Guadiana. Vertical lines indicate the location of the upper and lower tercile values of the streamflow series.

lower, and middle terciles of the third autumn SST PC series were computed. Composites values for JFM streamflows following upper tercile SST anomalies were -0.30 for the Douro, -0.31 for the Tejo, and -0.26 for the Guadiana. For the three rivers, the difference between the upper tercile SST composite values and that of the middle and lower tercile proved to be statistically significant at the 95% confidence level using a t test.

To sum up, the previous results show the preference for negative streamflow anomalies following tropical Atlantic summer negative SST anomalies and following southwestern Atlantic autumn SST positive anomalies. The second summer SST PC and third autumn PC thus provide useful information for the seasonal forecasting of the winter streamflow series. But the nonlinear nature of this information makes it particularly difficult to incorporate it in the framework of a forecasting system.

c. ARMA plus SST forecasting

Based on the previous section results and those obtained in the preceding companion paper (Part I), the following linear model can be proposed to represent the winter river flow series:

$$\text{raw river flow} = \text{ARMA} + \text{River_ARMA} + \varepsilon. \quad (1)$$

The first term on the right-hand side stands for the interannual linear predictable signal obtained based on the series history alone in Part I. The second term corresponds to the linear forecasting information provided by the autumn Atlantic SST, which can provide for the following winter streamflow. Therefore, this term stands for the seasonal forecast. The last term represents the error, that is, information that neither the interannual history of the series nor the previous season's Atlantic SST can provide.

A linear forecasting experiment was conducted using the model proposed in Eq. (1). In practice, the new forecasts were obtained by adding the results of the ARMA models, presented in Part I, and the results of the River_ARMA models obtained in section 3b(1). Figures 5, 6, and 7 present the results of these forecasting experiments for the Douro, Tejo, and Guadiana, respectively. Figures 5a, 6a, and 7a show the forecasts during the period 1930–85 for the Douro and Tejo and during the period 1953–85 for the Guadiana, while Figs. 5b, 6b, and 7b show the forecasts for the validation period 1986–2004. Tables 3, 4, and 5 summarize the performance skill obtained with these models. For the sake of comparison, the results of the forecasts based only on the ARMA models are also shown, both in the tables and in the figures.

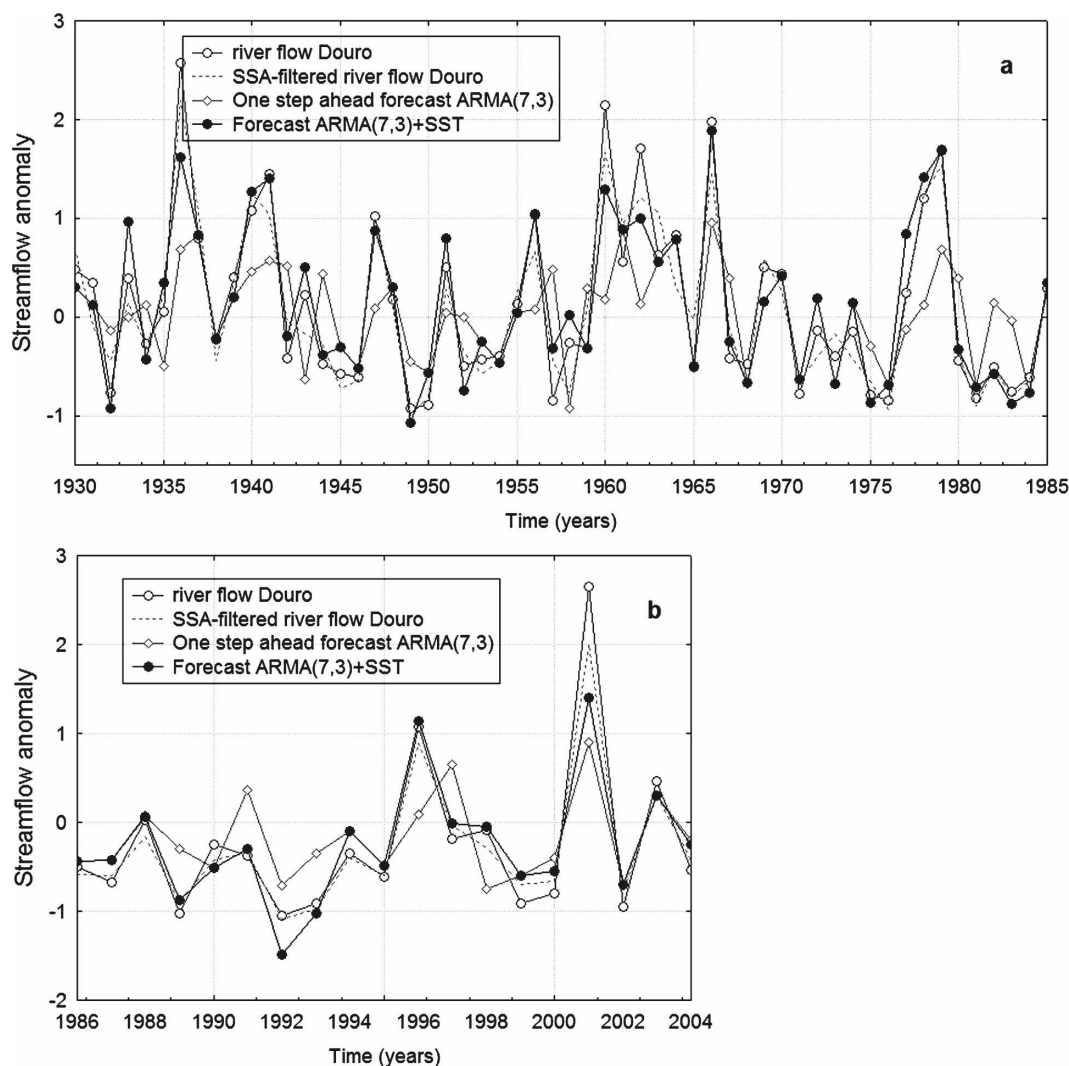


FIG. 5. Results of the forecasting experiment for the Douro streamflow series: (a) one-step-ahead forecasts using both the ARMA-alone and the ARMA+SST model for the calibration period 1923–85; (b) as in (a), but for the validation period 1986–2004. The SSA-filtered river flow series and the raw (unfiltered) streamflow series are also displayed.

Overall, the inclusion of the SST information improves the skill of the combined model forecasts when compared to the ARMA-alone model forecasts. This improvement is particularly impressive for the Douro and Guadiana and is minor for the Tejo. From the corresponding figures, one can state that the ARMA-alone models tend to underestimate the extreme positive streamflow values. This is also true for the extreme negative values, although in these cases the difference is smaller. It is worth mentioning that the SST information is able, in many cases, to modify the ARMA-alone estimates in the correct way. As a consequence, by including the upgrading SST information, the model forecast skill increases considerably.

The Douro River shows a considerable improvement in the forecasting skill by using the SST information (Table 3). In particular, during the validation period, the improvement against climatology is 88%, and 95% against persistence; while the ARMA-alone forecast provides an improvement of 51% and 75%, respectively. Additionally, the correlation coefficient is 0.93 (0.73 using only the ARMA model), which means that the combined model can explain 86% of the variability. Finally, the phase agreement is 95% (90% using the ARMA model). Skill values are very similar during the calibration period. A close look at Figs. 5a and 5b reveals the years responsible for these improvements in the skill parameters. The ARMA-alone model tends to

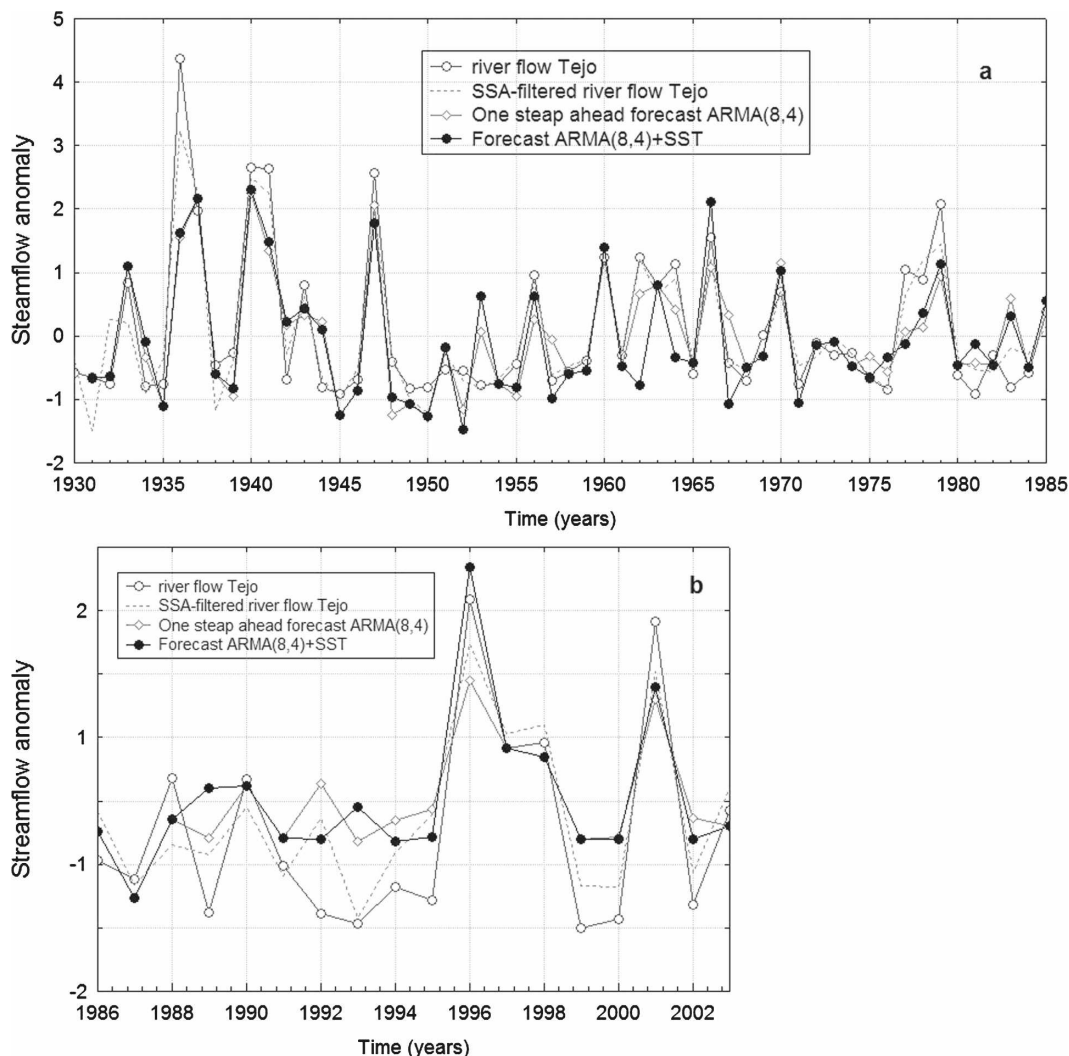


FIG. 6. As in Fig. 5, but for the Tejo River.

underestimate the extreme positive values and provides a relatively poor forecast for extreme negative values. The use of the SST information significantly offsets both pitfalls, providing better estimates for positive (e.g., 1996, 2001) and negative (e.g., 1989, 1992) extreme values during the validation period, or 1975–85 during the calibration period.

The Tejo River shows the lowest improvement, among the three rivers, in forecasting skill using the SST information. During the validation period 1986–2004, the model performs around 61% better than climatology, 68% better than persistence, using the SST information (Table 4); when using only the ARMA model, the improvements are 53% and 68%, respectively. This implies a small increment against climatology and no increment at all against persistence. As shown in Fig. 6b, this slight improvement against cli-

matology has to do mainly with the better capacity to forecast extreme positive values. In these cases (e.g., 1996 and 2001), the SST information provides valuable additional information in order to improve the estimates from the ARMA-alone model. This is also true for the calibration period during which a slight increment in the skill of the model against climatology is obtained (see, e.g., 1956, 1970, 1979, and 1983). On the other hand, for the extreme negative streamflow values, the use of the SST information does not seem to improve model skill. Overall, the phase accordance of the model with the observations is around 90% during the validation period and the correlation coefficient is 0.89, showing that the model is able to explain around 73% of the winter Tejo streamflow variability during the period 1986–2004 (Table 4).

Results for the Guadiana River are similar to those

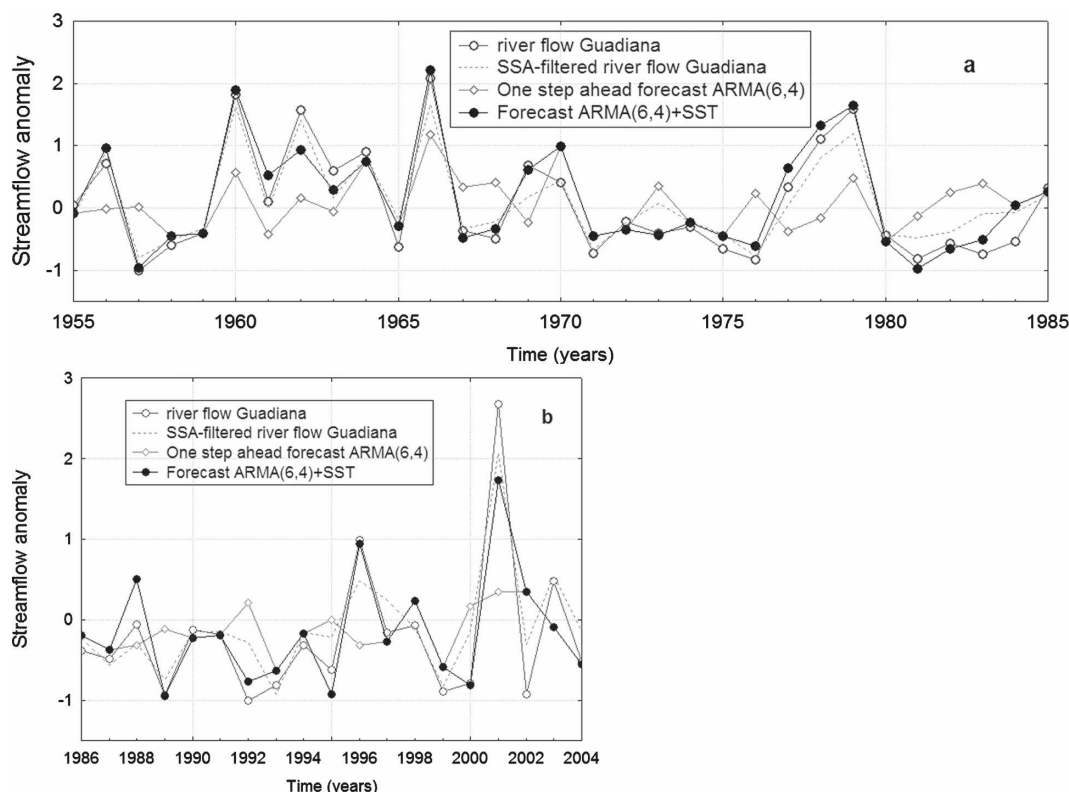


FIG. 7. As in Fig. 5, but for the Guadiana River.

obtained for the Douro. Using the SST information the forecast skill measures improve significantly. In particular, during the validation period, the improvement against climatology and persistence is now, respectively, 90% and 96%, being limited to 52% and 81% when we use the ARMA-alone model. Similar values can be found for the calibration period. It is particularly worth stressing the improvement against climatology. Similarly, the correlation coefficient also improves, from 0.47 using the ARMA-alone model to 0.90 using

the combined model, explaining around 80% of the streamflow variability. Again, the main reason for the improvement in forecasting skills of the complete model is that the SSTs provide better estimates for both the extreme positive (e.g., 1996, 2001) and negative (e.g., 1989, 1992, 2000) streamflow values during the validation period, or 1975–85 during the calibration period (Figs. 7a and 7b).

To sum up, the SST information improves the forecasts, particularly for the Douro and Guadiana Rivers.

TABLE 3. Statistical results for the Douro streamflow forecasting experiment using both the ARMA and regression model, which includes SST information. Results are displayed both for the calibration and validation period. For comparison, the results of the ARMA-alone forecast are also shown. Correlation coefficients, r , with an asterisk are statistically significant at the 95% confidence level.

	Calibration (1930–85)		Validation (1986–2004)	
	One-step-ahead ARMA	One-step-ahead ARMA and SST	One-step-ahead ARMA	One-step-ahead ARMA and SST
MSE	0.48	0.08	0.38	0.09
MAE	0.52	0.19	0.47	0.18
r	0.60*	0.94*	0.73*	0.93*
MSE_{cli}		0.77		0.77
MSE_{per}		1.35		1.88
$SMSE_{cli}$ (%)	37	90	51	88
$SMSE_{per}$ (%)	61	95	79	95
Phase accordance (%)	80	97	90	95

TABLE 4. As in Table 3, but for the Tejo River.

	1931–85		1986–2004	
	One-step-ahead ARMA	One-step-ahead ARMA and SST	One-step-ahead ARMA	One-step-ahead ARMA and SST
MSE	0.43	0.18	0.26	0.23
MAE	0.47	0.29	0.43	0.40
r	0.83*	0.80*	0.85*	0.89*
MSE _{cli}		0.69		0.59
MSE _{per}		1.43		1.28
SMSE _{cli} (%)	38	40	53	61
SMSE _{per} (%)	67	66	68	68
Phase accordance (%)	89	90	90	90

These two rivers seem to be especially sensible to the autumn SST variability over those regions represented by the second autumn PC, that is, the so-called North Atlantic horseshoe pattern.

4. Discussion and concluding remarks

The role of the Atlantic SST on the seasonal predictability of winter Iberian Peninsula river flows is analyzed for the period 1923–2004. The analysis was built upon the output results obtained with the interannual predictability experiment carried out in the companion paper (Part I). In this follow-up work, the main aim was to study the additional skill provided by the Atlantic summer and autumn SSTs in order to forecast the part of winter streamflow variability that an interannual ARMA forecasting model was incapable of capturing. To this end, a standard PCA was applied for the entire Atlantic Ocean summer and autumn SSTs. Then, the association between the resulting principal component series and the streamflow series was analyzed in order to use the PC series as predictor variables in a linear seasonal forecasting regression model. A nonlinear analysis of the relationship between the SSTs and the streamflow series was also performed. Finally, the results of the linear seasonal regression models were in-

tegrated with the results of the interannual model obtained in Part I.

Results showed several important facts: first, only the second autumn mode has a statistically significant linear influence on the variability of the following winter streamflow values. This mode shows a tripole spatial pattern of anomalies in the North Atlantic area, which is commonly called the North Atlantic horseshoe. The inclusion of this SST information improves the skills of the forecasts compared to the ARMA-alone model forecasts. The improvement against climatology ranges from 61% to 90% (51% to 53% when using the ARMA-alone approach). These improvements are mostly related to the ability of the SST information to provide better estimates of the extreme positive streamflow values. Additionally, the second summer mode, which represents the tropical Atlantic SST variability, and the third autumn mode, which accounts for the southwestern Atlantic area, have a significant nonlinear influence on the following winter streamflow values. In particular, there is a tendency for negative winter streamflow anomalies following negative SSTs anomalies in the area of the second summer mode. There is also a tendency for negative winter streamflow anomalies following positive SSTs anomalies in the area of the third autumn mode.

TABLE 5. As in Table 3, but for the Guadiana River.

	1953–85		1986–2004	
	One-step-ahead ARMA forecasting model	One-step-ahead ARMA and SST forecasting model	One-step-ahead ARMA forecasting model	One-step-ahead ARMA and SST forecasting model
MSE	0.36	0.08	0.34	0.07
MAE	0.41	0.21	0.41	0.18
r	0.48*	0.95*	0.47*	0.90*
MSE _{cli}		0.68		0.72
MSE _{per}		0.67		1.82
SMSE _{cli} (%)	47	88	52	90
SMSE _{per} (%)	46	88	81	96
Phase accordance (%)	52	93	54	100

The former results can be summarized in the following way. The ARMA model provides the interannual linearly predictable signal contained in the history of the time series, which is, probably, mostly related to the Atlantic SST. But, there is also a considerable linear relationship between SST and winter streamflow in Iberia at seasonal time scales, particularly concerning the preceding autumn SST. It could be argued that the ARMA models provide the low-frequency (interannual) useful information for the forecast (which may result from the low-frequency relationship between the SST and the precipitation/streamflow fields). Additionally, the summer and autumn SSTs provide a “seasonal upgrade” of the state of the ocean, useful for the forecasts, related to physical phenomena that links the atmosphere and the ocean at seasonal time scales. Another overall outcome of this analysis is that the linear interannual predictability is considerably greater than the linear seasonal predictability. These comments apply for all three rivers analyzed. Using the improvement against climatology (Tables 3, 4, and 5) it seems reasonable to argue that the interannual linear predictability accounts for around two-thirds of the total predictability, while the seasonal one only accounts for the remaining third.

The extent to which the Atlantic SST anomalies exert an influence on the North Atlantic atmospheric circulation has been a topic of intense research in the last decades. Unfortunately, there is no general agreement on the extent and importance of this influence; moreover, its usefulness and reliability for seasonal climate forecasting has not yet been reached. Nevertheless, in recent years there is growing evidence of the existence of a lead-lag relationship of several months between SST anomaly patterns and the North Atlantic Oscillation (NAO), which could be useful for seasonal forecasts (Rodwell and Folland 2002; Czaja and Frankignoul 1999, 2002; Drévillon et al. 2001).

Czaja and Frankignoul (2002) found that the negative NAO winter pattern is preceded during summer and autumn by a horseshoe-like pan-Atlantic SST anomaly. This pattern is composed by a band of warm water in the midlatitude east Atlantic extending from the subpolar to the subtropical region and enclosing a cold SST anomaly off the east coast of the United States. Additionally, the pattern has a southern center in the equatorial Atlantic, with positive SST anomaly between 20°N and 20°S preceding the negative phase of the NAO. Although the mechanism for this ocean-atmosphere relationship has been widely analyzed (e.g., Czaja and Frankignoul 2002; Watanabe and Kimoto 2000; Cassou et al. 2004), the nature of the summer and autumn ocean influence on the next winter NAO is still

unclear. Czaja and Frankignoul (2002) also analyzed the relative roles of both centers of action in determining the winter NAO, and their results showed that the bulk of the signal comes from the midlatitudes. In general, it is considered that the tropical Atlantic has a weaker, but significant, impact on the NAO with warmer tropical SST preceding a negative NAO phase by 1–2 months. However, in a recent work, Peng et al. (2005) also evaluated, using a general circulation model, the role of both the North Atlantic and equatorial Atlantic components of the pan-Atlantic summer and autumn SST anomaly in determining the following winter NAO. Their results showed that the equatorial pattern is most important in forcing the winter NAO, with positive anomalies preceding negative NAO winter. It seems, therefore, that there is a weak but significant response of the winter NAO to previous summer and autumn SSTs over the Atlantic at both middle latitudes and the equatorial belt. Roughly, the first summer and second autumn SST PCs found in this work (Figs. 1a and 2b) resemble the northern (central and North Atlantic) part of the horseshoe-like pan-Atlantic SST anomaly. Additionally, the second summer and first autumn PCs (Figs. 1b and 2a) bear a resemblance to the southern (tropical Atlantic) part (see, e.g., Fig. 9 in Czaja and Frankignoul 2002 and Fig. 1 in Peng et al. 2005).

Based on this association, results in section 3b are in good agreement with the previously discussed influence of the summer and autumn SST in the following winter NAO. In particular, the spatial pattern represented in Fig. 2b is associated with the negative phase of the NAO. Therefore, the positive correlation between the second autumn PCs and the following winter streamflow series can be related to this phase of the NAO, which leads to positive precipitation (and streamflow) anomalies in Iberia. The opposite SST anomalies lead to the positive phase of the NAO and, then, to negative precipitation and streamflow anomalies. We have shown that the improvements in the forecasting skill provided by the second autumn SST PC series was mostly associated with better estimates of the extreme streamflow values. Then, it could be concluded that the autumn SST variability of the Atlantic horseshoe pattern has some kind of shifting effect of the “normal” precipitation regime over the Iberian Peninsula during the following winter. This effect leads to changes in the variability rather than in the mean. This influence is mainly present in the Guadiana River basin. The Guadiana basin is the southernmost of the three rivers and the precipitation, strongly related to the NAO, presents a strong interannual variability. Overall, the previous result agrees with similar works carried out for the Ibe-

rian Peninsula. For instance, Rodríguez-Fonseca and de Castro (2002) and Rodríguez-Fonseca et al. (2006) analyzed the influence of the Atlantic SST on the Iberian Peninsula winter precipitation. They found that the summer SST anomalies in the subtropical Atlantic between 10° and 30°N are positively correlated with the following winter precipitation over the Iberian Peninsula and northern Africa, while a negative correlation is found for the SST around 45°. This pattern roughly represents the northern part of the horseshoe-like pattern. Additionally, in a recent paper, Rimbu et al. (2005) evaluated the seasonal predictability of the Danube streamflow based on SST. Results showed that a significant part of the Danube winter streamflow can be predicted based on the previous autumn SST values of certain areas in the North Atlantic, particularly the southern part of the North Atlantic horseshoe pattern.

The nonlinear influence of the second summer SST PC on the following winter streamflow found in this work can be explained based on the previously discussed SST–NAO relationship. In particular, the positive/negative summer SSTs anomalies are associated with negative/positive NAO, and therefore positive/negative streamflow series. Results of our analysis show that this influence is significant only during negative SST anomalies; no significant counterpart relationship is found during positive SST anomalies. Additionally, our results indicate that this relationship between tropical Atlantic summer SST and winter streamflow vanishes throughout the autumn months. The existence of a nonlinear relationship between summer and autumn SST and the following winter Iberian streamflow may be associated with the asymmetry of the precipitation processes. The precipitation regime of the Iberian Peninsula has a highly irregular behavior in both spatial and temporal scales (Esteban-Parra et al. 1998; Serrano et al. 1999; Trigo and DaCamara 2000). Winter and spring precipitation variability can be explained as a function of changes in large-scale modes at monthly scales, especially over the western sector of the Iberian Peninsula (Trigo and Palutikof 2001; Goodess and Jones 2002). Frontal activity, cyclones, or troughs of lower pressure are usually associated with precipitation in Iberia (Zorita et al. 1992; Rodríguez-Puebla et al. 1998). On the other hand, dry spells in Iberia are associated mainly with blocking by the Azores high. The associated counterpart SST patterns of variability in the Atlantic Ocean are not necessarily opposite to each other.

To sum up, our results suggest that the two competing oceanic influences on the NAO (one from the mid-latitudes, the other from the tropics), induce a different response on the NAO mode: a linear one from the

midlatitudes, which is more important in autumn, and a nonlinear one from the tropics, which is more important during summer and during negative SST anomalies in the tropical Atlantic. From a pure operational point of view, the model described in this study presents the pitfall of using autumn (SON) SST data to predict winter (JFM) streamflow: This amounts to only a one-month lag between predictor and predictand. Nevertheless, the feasibility of developing a seasonal statistical forecasting system for the Iberian Peninsula river streamflow has been proved, which may improve the management of the increasing limited water resources in this region.

Acknowledgments. The Spanish Ministry of Education and Science, Research Projects CGL2004-05340-C02-01/CL1 and CGL2007-61151/CL1, financed this study. R. M. Trigo was supported by the Portuguese Science Foundation (FCT) through project PREDATOR (Seasonal Predictability and Downscaling over the Atlantic European Region), Contract POCI/CTE-ATM/62475/2003. River flow data from Douro, Tejo, and Guadiana were kindly provided by Instituto Nacional da Água (INAG). The UKMO GISST 2.2 data were kindly provided by the British Atmospheric Data Centre, Rutherford Appleton Laboratory, Chilton, United Kingdom. The authors would like to express their sincere thanks to Dr. Carlos Pires, University of Lisbon (Portugal), and the anonymous reviewers who provided very useful comments on an earlier version of this manuscript.

REFERENCES

- Box, G. E. P., and G. M. Jenkins, 1976: *Time Series Analysis: Forecasting and Control*. Holden-Day, 543 pp.
- Cassou, C., C. Deser, L. Terray, J. Hurrell, and M. Drévilion, 2004: Summer sea surface temperature conditions in the North Atlantic and their impact upon the atmospheric circulation in early winter. *J. Climate*, **17**, 3349–3363.
- Coelho, C., D. Stephenson, F. J. Doblas-Reyes, M. Balmaseda, A. Guetter, and G. J. van Oldenborgh, 2006: A Bayesian approach for multi-model downscaling: Seasonal forecasting of regional rainfall and river flows in South America. *Meteor. Appl.*, **13**, 73–82.
- Colman, A., and M. Davey, 1999: Prediction of the summer temperature, precipitation and pressure in Europe from preceding winter North Atlantic Ocean temperatures. *Int. J. Climatol.*, **19**, 513–536.
- Czaja, A., and C. Frankignoul, 1999: Influence of the North Atlantic SST on the atmospheric circulation. *Geophys. Res. Lett.*, **26**, 2969–2972.
- , and —, 2002: Observed impact of Atlantic SST anomalies on the North Atlantic Oscillation. *J. Climate*, **15**, 606–623.
- Drévilion, M., L. Terray, P. Rogel, and C. Cassou, 2001: Mid latitude Atlantic SST influence on European winter climate variability in the NCEP reanalysis. *Climate Dyn.*, **18**, 331–344.
- Esteban-Parra, M. J., F. S. Rodrigo, and Y. Castro-Díez, 1998: Spatial and temporal patterns of precipitation in Spain for the period 1880–1992. *Int. J. Climatol.*, **18**, 1557–1574.

- Gámiz-Fortis, S. R., D. Pozo-Vázquez, R. M. Trigo, and Y. Castro-Díez, 2008: Quantifying the predictability of winter river flow in Iberia. Part I: Interannual predictability. *J. Climate*, **21**, 2484–2502.
- Goodess, C. M., and P. D. Jones, 2002: Links between circulation and changes in the characteristics of Iberian rainfall. *Int. J. Climatol.*, **22**, 1593–1615.
- Hartmann, H. C., T. C. Pagano, S. Sorooshian, and R. Bales, 2002: Confidence builders: Evaluating seasonal climate forecasts from user perspectives. *Bull. Amer. Meteor. Soc.*, **83**, 683–698.
- Hipel, K. W., and A. I. McLeod, 1994: *Time Series Modelling of Water Resources and Environmental Systems*. Elsevier, 1013 pp.
- Liang, X., D. P. Lettenmaier, E. F. Wood, and S. J. Burges, 1994: A simple hydrologically based model of land surface water and energy fluxes for GSMs. *J. Geophys. Res.*, **99** (D7), 14 415–14 428.
- Lloyd-Hughes, B., and M. A. Saunders, 2002: Seasonal prediction of European spring precipitation from El Niño–Southern Oscillation and local sea-surface temperatures. *Int. J. Climatol.*, **22**, 1–14.
- Mariotti, A., N. Zeng, and K. M. Lau, 2002: Euro-Mediterranean rainfall and ENSO—A seasonally varying relationship. *Geophys. Res. Lett.*, **29**, 1621, doi:10.1029/2001GL014248.
- Nigam, S., M. Barlow, and E. Berbery, 1999: Analysis links Pacific decadal variability to drought and streamflow in United States. *Eos, Trans. Amer. Geophys. Union*, **80**, 621–622.
- North, G. R., T. L. Bell, R. F. Cahalan, and F. J. Moeng, 1982: Sampling errors in the estimation of empirical orthogonal functions. *Mon. Wea. Rev.*, **110**, 699–706.
- Phillips, I., and G. R. McGregor, 2002: The relationship between monthly and seasonal south-west England rainfall anomalies and concurrent North Atlantic sea surface temperature. *Int. J. Climatol.*, **22**, 197–217.
- Peng, S., W. Robison, S. Li, and M. P. Hoerling, 2005: Tropical Atlantic forcing of coupled North Atlantic seasonal responses. *J. Climate*, **18**, 480–496.
- Piechota, T. C., J. A. Dracup, and R. G. Fovell, 1997: Western U.S. streamflow and atmospheric circulation patterns during El Niño–Southern Oscillation. *J. Hydrol.*, **201**, 249–271.
- Pozo-Vázquez, D., M. J. Esteban-Parra, F. S. Rodrigo, and Y. Castro-Díez, 2001: The association between ENSO and winter atmospheric circulation and temperature in the North Atlantic region. *J. Climate*, **16**, 3408–3420.
- , S. R. Gámiz-Fortis, J. Tovar-Pescador, M. J. Esteban-Parra, and Y. Castro-Díez, 2005: North Atlantic winter SLP anomalies based on the autumn ENSO state. *J. Climate*, **18**, 97–103.
- Preisendorfer, R. W., 1988: *Principal Components Analysis in Meteorology and Oceanography*. Elsevier, 419 pp.
- Rajagopalan, B., M. E. Mann, and U. Lall, 1998: A multivariate frequency-domain approach to long-lead climatic forecasting. *Wea. Forecasting*, **13**, 58–74.
- Rasmusson, E. M., and T. H. Carpenter, 1982: Variations in tropical sea surface temperature and surface wind fields associated with the Southern Oscillation/El Niño. *Mon. Wea. Rev.*, **110**, 354–384.
- Redmond, K., and R. Koch, 1991: Surface climate and streamflow variability in Western United States and their relationship to large-scale circulation indices. *Water Resour. Res.*, **27**, 2381–2399.
- Rimbu, N., M. Dima, G. Lohmann, and S. Stefan, 2004: Impacts of the North Atlantic Oscillation and the El Niño–Southern Oscillation on Danube river flow variability. *Geophys. Res. Lett.*, **31**, L23203, doi:10.1029/2004GL020559.
- , —, —, and I. Musat, 2005: Seasonal prediction of Danube flow variability based on stable teleconnection with sea surface temperature. *Geophys. Res. Lett.*, **32**, L21704, doi:10.1029/2005GL024241.
- Rodriguez-Fonseca, B., and M. de Castro, 2002: On the connection between winter anomalous precipitation in the Iberian Peninsula and north west Africa and summer subtropical Atlantic sea surface temperature. *Geophys. Res. Lett.*, **29**, 1863, doi:10.1029/2001GL014421.
- , I. Polo, E. Serrano, and M. de Castro, 2006: Evaluation of the North Atlantic SST forcing on the European and northern Africa winter climate. *Int. J. Climatol.*, **26**, 179–191.
- Rodriguez-Puebla, C., A. H. Encinas, S. Nieto, and J. Garmendia, 1998: Spatial and temporal patterns of annual precipitation variability over the Iberian Peninsula. *Int. J. Climatol.*, **18**, 299–316.
- Rodwell, M. J., and C. K. Folland, 2002: Atlantic air-sea interaction and seasonal predictability. *Quart. J. Roy. Meteor. Soc.*, **128**, 1413–1443.
- , D. P. Rowell, and C. K. Folland, 1999: Oceanic forcing of the wintertime North Atlantic Oscillation and European climate. *Nature*, **398**, 320–323.
- Saunders, M. A., and B. Qian, 2002: Seasonal predictability of the winter NAO from North Atlantic sea surface temperatures. *Geophys. Res. Lett.*, **29**, 2049, doi:10.1029/2002GL014952.
- Serrano, A., A. J. Garcia, V. L. Mateos, M. L. Cancillo, and J. Garrido, 1999: Monthly modes of variation of precipitation over the Iberian Peninsula. *J. Climate*, **12**, 2894–2919.
- Trigo, R. M., and C. C. DaCamara, 2000: Circulation weather types and their impact on the precipitation regime in Portugal. *Int. J. Climatol.*, **20**, 1559–1581.
- , and J. P. Palutikof, 2001: Precipitation scenarios over Iberia: A comparison between direct GCM output and different downscaling techniques. *J. Climate*, **14**, 4422–4446.
- van Oldenborgh, G. J., G. Burgers, and A. K. Tank, 2000: On the El Niño teleconnection to spring precipitation in Europe. *Int. J. Climatol.*, **20**, 565–574.
- Vicente-Serrano, S. M., 2005: El Niño and La Niña influence on droughts at different timescales in the Iberian Peninsula. *Water Resour. Res.*, **41**, W12415, doi:10.1029/2004WR003908.
- Watanabe, M., and M. Kimoto, 2000: Atmosphere-ocean thermal coupling in the North Atlantic: A positive feedback. *Quart. J. Roy. Meteor. Soc.*, **126**, 3343–3369.
- Wedgbrow, C., R. Wilby, H. Fox, and G. O'Hare, 2002: Prospects for seasonal forecasting of summer drought and low river flow in England and Wales. *Int. J. Climatol.*, **22**, 219–236.
- Wilby, R., 1993: Evidence of ENSO in the synoptic climate of the British Isles since 1880. *Weather*, **48**, 234–239.
- , 2001: Seasonal forecasting of river flows in the British Isles using North Atlantic pressure patterns. *J. Chart. Inst. Water. Environ. Manage.*, **15**, 56–63.
- , C. S. Wedgbrow, and H. R. Fox, 2004: Seasonal predictability of the summer hydrometeorology of the River Thames, UK. *J. Hydrol.*, **295**, 1–16.
- Wilks, D. D., 1995: *Statistical Methods in the Atmospheric Sciences*. Academic Press, 467 pp.
- Zorita, E., V. Kharin, and H. von Storch, 1992: The atmospheric circulation and sea surface temperature in the North Atlantic area in winter: Their interaction and relevance for Iberian precipitation. *J. Climate*, **5**, 1097–1108.